Integration
geoscience
engineering
partnership
geoConvention 2013

The Design and Application of Converted-wave COVs

Richard Bale*, Key Seismic Solutions Ltd., Calgary, Canada.
Richard.Bale@keyseismic.com
Tobin Marchand, Keith Wilkinson and Jeff Deere, Key Seismic Solutions Ltd., Calgary, Canada.

Summary

We demonstrate an adaptation of the COV concept to converted-wave (PS) data, and discuss applications of the COV domain in PS processing. We illustrate that one possible application is to update the Vp/Vs used for CCP binning, based upon analysis of reciprocal COVs, with equal but opposite offset vector directions.

Introduction

There has been a spirited debate in the land seismic processing community on the relative merits of representing azimuthal information by azimuthal sectoring or by using the concept of the "Common Offset Vector" (COV) (Cary, 1999), also known at the "Offset Vector Tile" (OVT), (Vermeer, 2002). While both approaches have value, one of the most important arguments in favour of the COV approach is that, by a proper choice of sampling of the inline and crossline offset coordinates, each COV constitutes a single fold dataset covering the survey area – at least in the case of an ideal orthogonal acquisition geometry. The appropriate COV sampling choice is simply twice the receiver line interval in one direction and twice the shot line interval in the other, which lead naturally to a tiling of the inline/crossline plane with rectangular common midpoint patches.

However, for PS data the coverage is represented not by CMP locations, but by "Common Conversion Point" (CCP) locations. The true CCP locations are a function of offset, depth and the Vp/Vs ratio, with further complications for anisotropy. A simple approximation which is used for much preliminary PS processing is to neglect the depth dependence and use the "Asymptotic Conversion Point" or ACP locations.

The ACP coverage for a single cross-spread is compared with the corresponding CMP coverage in figure 1. The asymmetry of the ACP domain results in a compression of the coverage towards the receiver line, and an expansion away from the shot line.

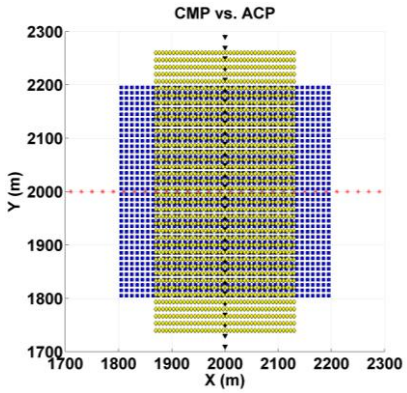

Figure 1. Comparison of CMP positions (blue) and ACP positions (yellow) for a single cross-spread with 40 shots (red stars) and 40 receivers (black triangles). Not all shots and receivers are shown.

Converted-wave COVs

If the same criterion is used for COV construction as for the P-wave case, then the corresponding ACP coverage is no longer single fold. There are two separate problems. First of all, the ACP locations do not fall on the same bin centres defined by CMP geometry. This can lead to a well-known periodicity of the total ACP fold (Eaton and Lawton, 1992). We regard this as a minor irritation from the COV point of view. The more fundamental problem is that the ACP tiles are a different shape to the CMP tiles, and do not uniformly cover the survey area: instead we have gaps in the shot line direction and overlaps in the receiver line direction (Vermeer, 2002). We have derived a simple correction for this problem involving a modification of the COV definitions based on the Vp/Vs ratio, to restore the tiling property of the COVs.

Letting the Vp/Vs ratio be denoted by γ, and the source-receiver offset vector by $\mathbf{r}$, then the asymptotic conversion point vector is given by (Fromm et al, 1985):

$$\mathbf{r}_{acp} = \frac{\gamma}{1+\gamma}\mathbf{r} \qquad (1)$$

If we assume that the shot lines are oriented parallel to the x-axis and the receiver lines parallel to the y-axis, then the offset X and Y grid intervals required for COVs to accommodate binning via equation (1) are:

$$C_x = (1+\gamma)\,\Delta R\,, \qquad (2a)$$

and

$$C_y = \left(\frac{1+\gamma}{\gamma}\right)\Delta S\,, \qquad (2b)$$

where ΔS and ΔR are the shot and receiver line intervals respectively. Obviously, if we set $\gamma = 1$, we recover the conventional PP criterion of twice line spacing.

In figure 2, we compare the COV tiling patterns for a given X-offset and Y-offset range. As stated previously, the increment of X and Y offsets required for uniform CMP coverage is twice the receiver- and shot-line increments. For the example in figure 2a we examine the CMP coverage for a COV that corresponds to an X-offset range from $2\Delta R$ to $4\Delta R$, and a Y-offset range from $2\Delta S$ to $4\Delta S$.

Figure 2a shows an “elementary tile” for this COV with CMP coverage for a single shot line running in the X direction (red stars), and a single receiver line running in the Y direction (black triangles). Figure 2d shows the CMP coverage for the 9 tiles which result from 3 shot lines and 3 receiver lines. For this conventional COV with CMP geometry, the tiles exactly cover the area with uniform single fold and no gaps or overlap, as is well known.

Figure 2b shows the elementary tile for ACP coverage using the standard COV definition, whereas figure 2c shows the elementary tile for ACP coverage using our modified sampling criterion of equation 2 for the COV definition. Figures 2e and 2f show the resulting 9-tile coverage patterns with the 3 shot lines and 3 receiver lines.

For the conventional COV, but using ACP geometry (2e) there are gaps and overlaps in the tiles. For the COV definition adapted to the ACP geometry (2f) we have eliminated gaps and overlaps between tiles - though we still do not achieve uniform single fold coverage.

There are various potential uses of the PS COV data. The next section explores one of these.

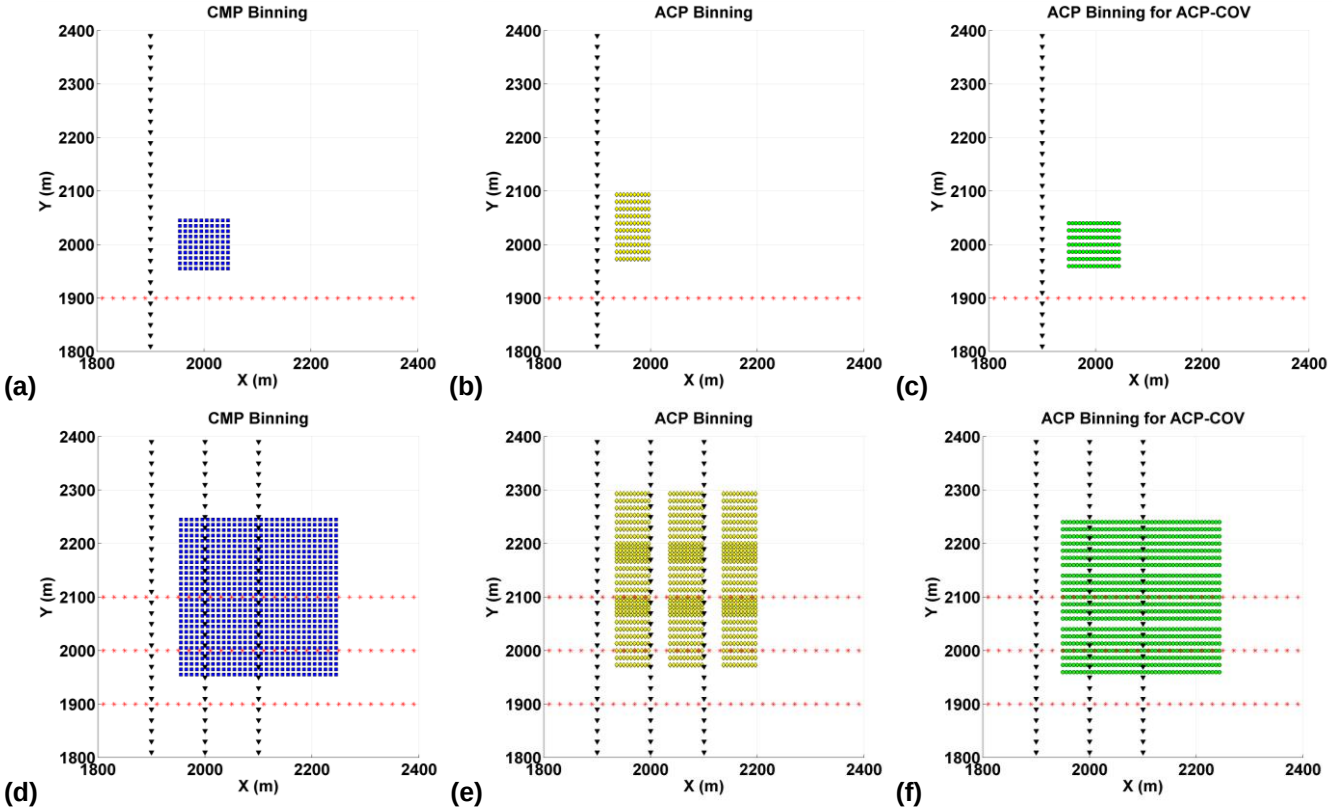

Figure 2. Comparison of COV coverage for a single COV: (a) and (d) CMPs using the standard COV definition; (b) and (e) ACPs using the standard COV definition; (c) and (f) ACPs using the PS-adapted COV definition. In (a), (b) and (c) a single tile from the COV, resulting from one cross-spread, is shown. In (d), (e) and (f), the 9 tiles resulting from three shot lines and three receiver lines are shown. The Vp/Vs ratio is 2 for the ACP cases.

Application to Converted-wave Binning

One application which is somewhat unique to PS data is the use of reciprocal COVs to check for alignment of data in CCP binning. For 2-D PS data, this is simply the comparison of positive and negative offset data which was first described by Audebert et al (1999). For 3-D, the action of CCP correction moves the trace along the shot-receiver azimuthal direction. It therefore is natural to choose reciprocal offset vectors for comparison. The misalignment of two images can be assessed and used to improve the choice of Vp/Vs for restacking with updated CCP correction.

This is illustrated using synthetic data generated for a real 3-D land orthogonal geometry. The synthetic is designed as a cross shape inside a circle forming a “target” (see prestack migrated time slice in Figure 7(a)). We will be using ACP corrections to compare different COV subsets of the data. It should be noted that the Vp/Vs values used to generate optimal ACP stacks are not representative of the true Vp/Vs, due to the limitations of the ACP approximation.

Figure 3 shows the COV grid (X and Y offsets) defined for (a) conventional CMP binning and (b) ACP binning with Vp/Vs=2. We will refer to the second as the PS COV. Figure 4 shows examples of the spatial fold variation for a single COV, corresponding to a near offset. Figure 4(a) is the CMP fold using the conventional COV of figure 3(a). Figure 4(b) is the ACP fold resulting from the same COV definition, and clearly illustrates the fold deficiencies which arise due to the asymmetry of the ACP domain – as described in the previous section. Compare this with figure 4(c) which is the ACP fold using the PS COV of figure 3(b). Though it is not possible to choose an exactly equivalent COV bin as

in figure 3(a), due to the different dimensions, we have chosen the bin which is most closely comparable. The improvement in coverage in figure 4 from (b) to (c) is quite apparent.

Turning now to the synthetic data, figure 5 shows a comparison of time slices at the target level from stacks using the conventional COV definition in (a) and (b). These two stacks form a reciprocal pair given by choosing equal but opposite X and Y offset bins. In the case of PP data these two would be equivalent: they can be, and often are, combined to improve the COV result. This is not allowed for PS: because the downward and upward modes are not the same, reciprocity cannot be applied, and so these pairs form distinct and different images. In fact the major difference observed is the spatial displacement between the centres of the targets, along the azimuthal direction for this COV. In figures 5 to 7, the true location of the centre of the target is indicated by the two faint diagonal lines. This displacement informs us that the Vp/Vs of 2 used to perform ACP binning (equation 1) in this case was not optimal to align the images. The corresponding reciprocal pair using the PS COV is shown in figure 5 (c) and (d). The improved continuity of the image, which results from the more uniform fold, allows a clearer analysis of the spatial displacement (about 930m) to update the Vp/Vs.

Similar to the method of Audebert et al. (1999), we have used this displacement to calculate a new "apparent" Vp/Vs of 4.2 which is optimal for ACP alignment. This has been applied, using equation 1, in figure 6. Of course, the new Vp/Vs for ACP binning has made the original PS COV design obsolete. It is best to redesign the COV binning with the new Vp/Vs ratio. In figure 6, (a) and (b) are the time slices from the ACP stacks with the original PS COV ($\gamma = 2$ in equation 2) whereas (c) and (d) are using an updated PS COV (we used $\gamma = 4$ in equation 2, approximating the ACP Vp/Vs of 4.2). The second pair of slices now have both good alignment - due to the updated Vp/Vs use in ACP binning – and improved coverage – due to the updated Vp/Vs used for PS COV design.

To illustrate the benefit of updating the Vp/Vs ratio to the final (unmigrated) stack, we compare in figure 7 the results of stacking all COVs using (b) the original Vp/Vs of 2, against (c) using the new Vp/Vs of 4.2. The correct (prestack migrated) image is shown in figure 7(a).

Discussion

For illustrative purposes we have restricted our study to the simplest of PS corrections, namely ACP binning. However, the potential use of the PS COV domain could certainly be extended to more advanced processing methods such as time-variant CCP stacking or to prestack time migration. As for PP data, the COV domain is very natural for azimuth preserving prestack migration of PS data, obviating the need for unnatural fold equalization prior to migration.

Likewise, just as for PP data, COVs are a natural goal of reconstruction methods, such as 5-D interpolation, where the reconstructed data can have source and/or receiver lines inserted between existing ones.

Conclusions

The COV concept can be modified for converted-wave data, to provide proper tiling under ACP geometry. Having done this, the converted-wave COVs become useful tools for applications such as updating Vp/Vs for binning corrections.

Acknowledgements

We thank Key Seismic Solutions for permission to publish this work. We thank Bernie Law and Doug Horton for their valuable assistance.

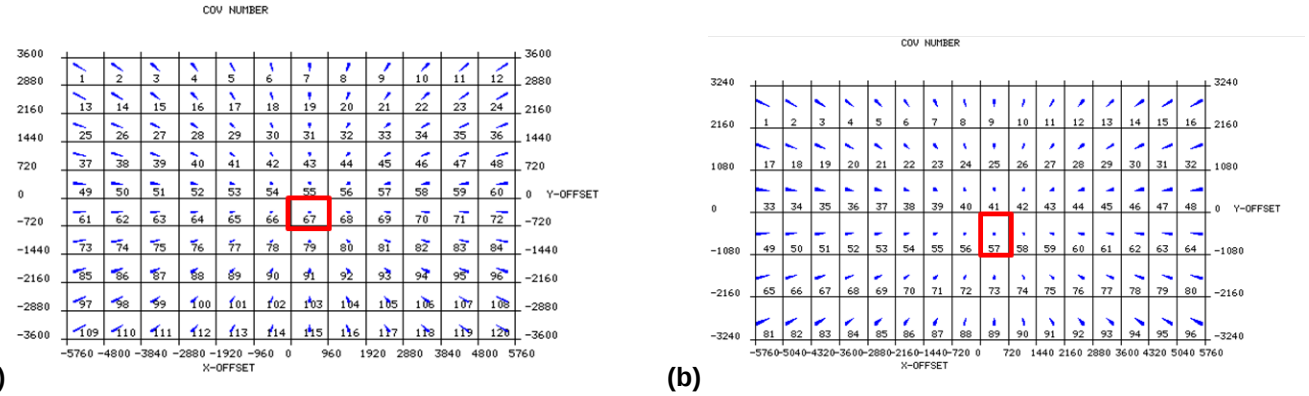

Figure 3. Gridding of X and Y offsets for different COV definitions. The horizontal axis is X offset, and the vertical axis is Y offset. Each cell represents a COV, with the number in the cell being a unique COV number and the blue vectors representing average offset and azimuth for each COV. The COV grids are shown for: (a) CMP geometry, and; (b) PS COV with ACP geometry with Vp/Vs=2. The offset bins identified by the red rectangles are used for the comparison of figure 4.

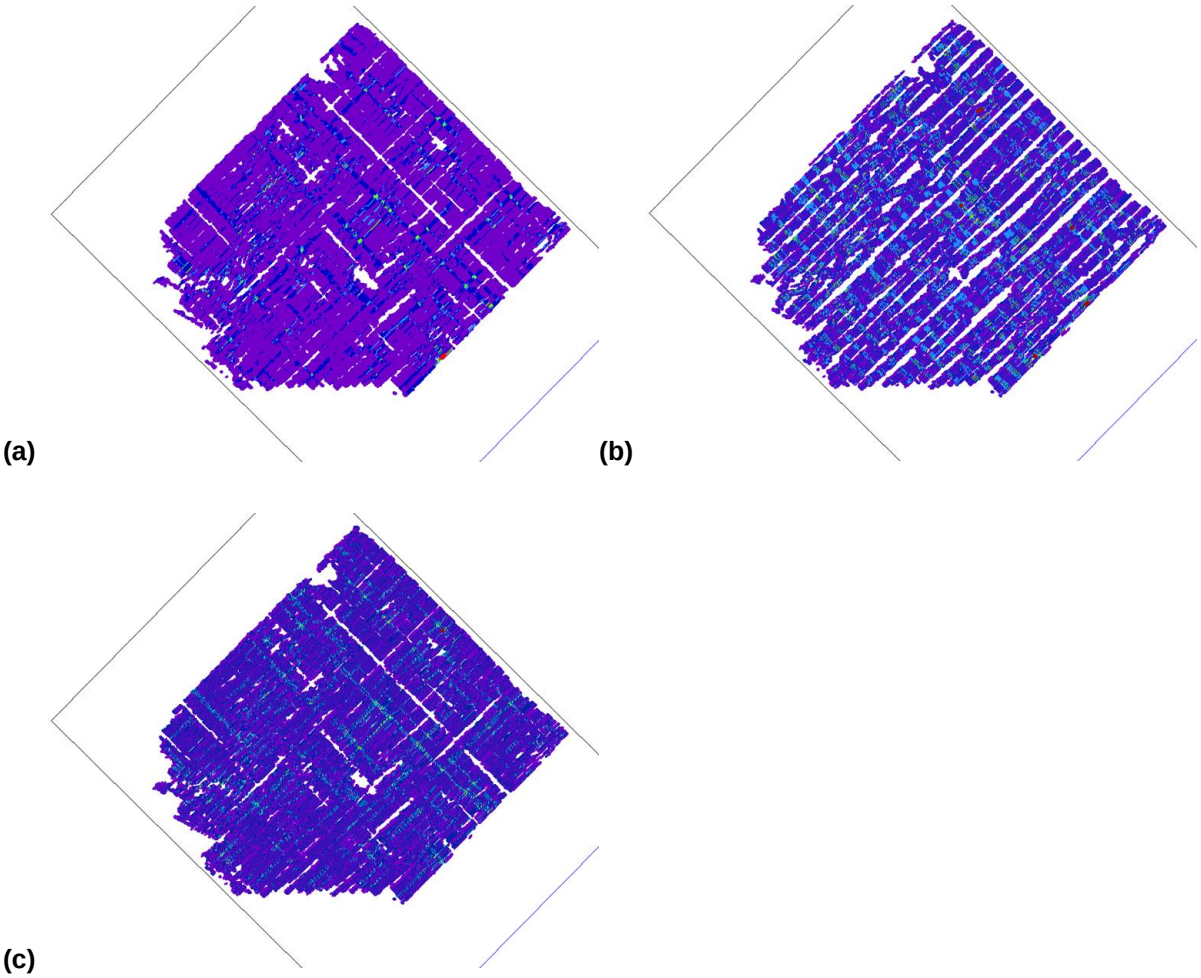

Figure 4. Single COV fold maps, with empty bins shown in white. The fold using CMP and ACP binning is shown in (a) and (b) for the conventional COV offset gridding definition, with X offset range [0m,960m) and Y offset range [-720m,0m), as shown in figure 3(a). Note the lack of uniform coverage for the ACP case. Figure 4(c) shows coverage for ACP binning after redefining COVs as in figure 3(b), using X offset range [0m,720m) and Y offset range [-1080m,0m).

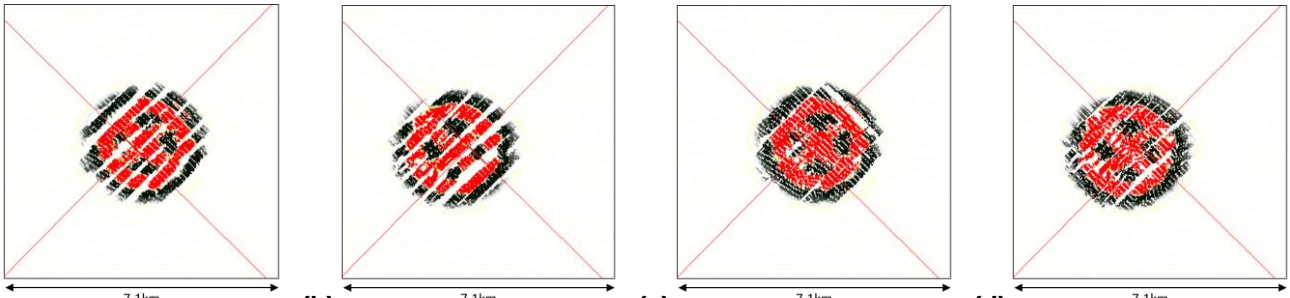

(a) (b) (c) (d)

Figure 5. Time slices through target from single COV stacks for PS synthetic, after ACP binning with Vp/Vs=2. The COV with X Offset range [-2880m,-1920m), Y offset range [1440m,2160m), is shown in (a) with its reciprocal COV shown in (b), using the conventional COV definition. The COV with X Offset range [-2880m,-2160m), Y offset range [1080m,2160m), and its reciprocal are shown in (c) and (d), using the PS COV definition.

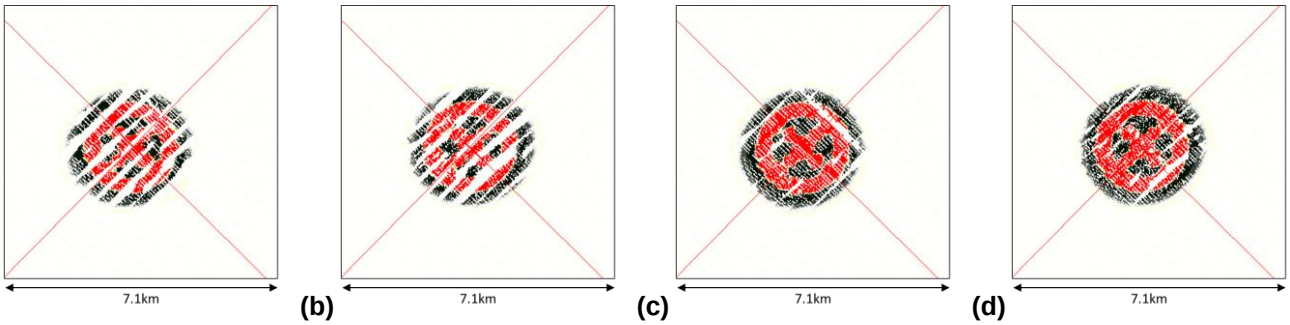

(a) (b) (c) (d)

Figure 6. Time slices through target from single COV stacks after ACP binning with Vp/Vs updated to 4.2, based on location mismatch from figure 5. (a) and (b) use PS COV defined for Vp/Vs =2 (same as used in figure 5(c) and (d)), whereas (c) and (d) are after redesigning COV for Vp/Vs=4.

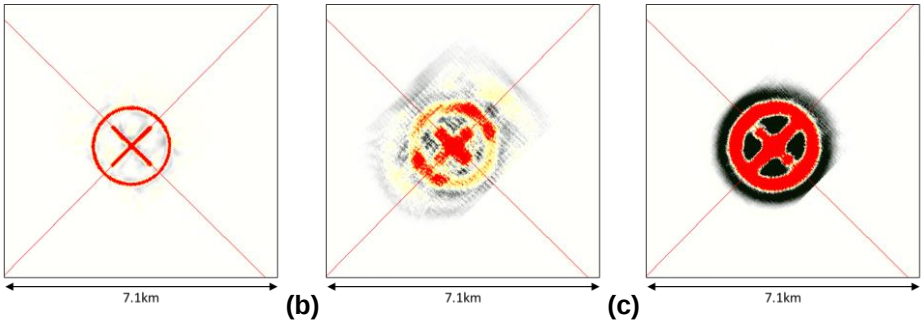

(a) (b) (c)

Figure 7. Comparison of time slices through target, from stacks using all of the data, for (a) prestack migrated data with correct model (b) original ACP stack using Vp/Vs=2 and (c) updated ACP stack with Vp/Vs = 4.2.

References

Audebert, F., Granger, P.Y., and Herrenschmidt, A., 1999, CCP-Scan technique: True common conversion point sorting and converted wave velocity analysis solved by PP and PS Pre-Stack Depth Migration: 69th Annual International Meeting, SEG, Expanded Abstracts, 1186-1189.

Cary, P., 1999, Common-offset-vector gathers: An alternative to cross-spreads for wide-azimuth 3-D surveys. SEG Technical Program Expanded Abstracts 1999: pp. 1496-1499.

Eaton, D. W. S., and Lawton, D.C., 1992, P-SV stacking charts and binning periodicity: Geophysics, 57, 745–748.

Fromm, G., Krey, T., and Wiest, B., 1985, Static and dynamic corrections, in Dohr, G., Ed., Seismic shear waves: Handbook of geophysical exploration, Geophys. Press, Vol. 15a, 191-225.

Vermeer, G. J. O., 2002, 3-D Seismic Survey Design: Geophysical References Series, SEG.